



Article

Impact of Titanium Oxide Nanoparticles on Growth, Pigment Content, Membrane Stability, DNA Damage, and Stress-Related Gene Expression in *Vicia faba* under Saline Conditions

Samar A. Omar ^{1,*}, Nabil I. Elsheery ², Pavel Pashkovskiy ³, Vladimir Kuznetsov ³, Suleyman I. Allakhverdiev ^{3,4,*} and Amina M. Zedan ⁵

¹ Genetics Department, Faculty of Agriculture, Tanta University, Tanta 31527, Egypt

² Agriculture Botany Department, Faculty of Agriculture, Tanta University, Tanta 31527, Egypt; nsheery@yahoo.com

³ K.A. Timiryazev Institute of Plant Physiology, Russian Academy of Sciences, Botanicheskaya Street 35, Moscow 127276, Russia; pashkovskiy.pavel@gmail.com (P.P.); vlkuzn@mail.ru (V.K.)

⁴ Faculty of Engineering and Natural Sciences, Bahcesehir University, Istanbul 34349, Turkey

⁵ Biological and Environmental Sciences Department, Faculty of Home Economics, Al-Azhar University, Cairo 11651, Egypt; aminazedan1948.el@azhar.edu.eg

* Correspondence: samar_omar5@agr.tanta.edu.eg (S.A.O.); suleyman.allakhverdiev@gmail.com (S.I.A.)

Abstract: This study investigates the effects of titanium dioxide nanoparticles ($n\text{TiO}_2$) on *Vicia faba* under salinity stress. Plants were treated with either 10 or 20 ppm $n\text{TiO}_2$ and subjected to two different concentrations of salinity (100 and 200 mM NaCl) as well as the combined effect of nanoparticles and salinity. Salinity induced a reduction in dry weight, increased electron leakage and MDA content, increased chromosomal aberrations and DNA damage, and reduced transcript levels of some stress- and growth-related genes. $n\text{TiO}_2$ treatment increased dry weight in unstressed plants and mitigated the salinity-damaging effect in stressed plants. $n\text{TiO}_2$ application improved cell division, decreased chromosomal aberrations, and reduced DNA damage in plants under saline conditions. The upregulation of antioxidant genes further supports the protective role of $n\text{TiO}_2$ against oxidative stress. Particularly significant was the ability of $n\text{TiO}_2$ to enhance the upregulation of heat shock protein (HSP) genes. These findings underscore the potential of $n\text{TiO}_2$ to reduce the osmotic and toxic effects of salinity-induced stress in plants.

Keywords: nanotitanium dioxide; salinity; chromosomal aberration; comet assay; antioxidant-encoding genes; heat shock proteins



Citation: Omar, S.A.; Elsheery, N.I.; Pashkovskiy, P.; Kuznetsov, V.; Allakhverdiev, S.I.; Zedan, A.M.

Impact of Titanium Oxide

Nanoparticles on Growth, Pigment Content, Membrane Stability, DNA Damage, and Stress-Related Gene Expression in *Vicia faba* under Saline Conditions. *Horticulturae* **2023**, *9*, 1030. <https://doi.org/10.3390/horticultrae9091030>

Academic Editor: Aisheng Xiong

Received: 6 August 2023

Revised: 8 September 2023

Accepted: 11 September 2023

Published: 13 September 2023



Copyright: © 2023 by the authors. Licensee MDPI, Basel, Switzerland. This article is an open access article distributed under the terms and conditions of the Creative Commons Attribution (CC BY) license (<https://creativecommons.org/licenses/by/4.0/>).

1. Introduction

Salinity stress is one of the primary abiotic stresses limiting plant growth and productivity in various parts of the world [1,2]. Approximately one-fifth of cultivated land worldwide (1500 million hectares) is salt-affected, which represents a great challenge for food security [3]. This is especially the case in Egypt, where the impacts of salinity are exacerbated due to factors such as excessive saltwater use in coastal areas, saline groundwater, and human-induced activities [4]. Salinity not only induces ion toxicity but also leads to the accumulation of reactive oxygen species (ROS), which in turn can damage cellular components through lipid peroxidation. This subsequently, has a cascade of harmful effects on the plant, including photosynthesis inhibition, changes in protein contents, enzyme activities, and modifications in nucleic acid content and structure. Consequently, the overall plant yield and productivity are significantly reduced under saline conditions [5,6]. The harmful impacts of salinity significantly reduce plant production under stress conditions [7,8]. *Vicia faba* is considered one of the cheapest sources of protein in the majority of developing countries [9]. *V. faba* is also recognized worldwide as an important crop in the animal feed market [10,11]. Egypt is one of the

major *V. faba* planting and producing countries, where it is considered a main source of essential nutrients due to the high protein content in its seed [9]. *V. faba*, a significant crop, particularly in Egypt, is unfortunately sensitive to salinity stress. This sensitivity leads to a substantial reduction in its yield, impacting its germination, growth, nodulation, and nitrogen fixation capabilities [12–14].

Because of the adverse effects of salinity in sensitive crops, numerous studies have recently focused on new strategies to mitigate its impacts on crop production [15,16]. Nanoparticles (NPs) have emerged as a promising tool to counteract the detrimental effects of salinity stress [17]. Nanoparticles create a particular type of material with a size of less than 100 nm [18]. Interactions between NPs and plant cells result in alterations in biological pathways and gene expression patterns, thus eventually affecting plant growth and development [19]. A variety of nanoparticles, including titanium oxide ($n\text{TiO}_2$), selenium oxide ($n\text{SeO}$), and zinc oxide ($n\text{ZnO}$), have been examined for their potential in stress amelioration and growth promotion in plants [20–22]. Among these, titanium oxide nanoparticles ($n\text{TiO}_2$) have gained prominence due to their potential in the agriculture and food industries. Scavenging ROS and stimulating antioxidant enzymes are the main roles of most studied nanoparticles [22–26]. Engineered nanotitanium dioxide ($n\text{TiO}_2$) largely produces NPs with multiple applications in the agriculture and food industries [27]. Recently, several studies have shown that $n\text{TiO}_2$ could enhance the growth and yield parameters of some plants under stress [28,29]. The primary mechanisms through which $n\text{TiO}_2$ exerts its beneficial effects include ROS scavenging and stimulating antioxidant enzyme activities. This can potentially help plants combat the oxidative damage posed by salinity. Furthermore, the transcriptional changes that $n\text{TiO}_2$ can bring about in plants, especially in response to stresses, are areas that are still largely unexplored [30].

While NPs have been studied extensively for their potential to alleviate various biotic and abiotic stresses in plants, the specific interaction between $n\text{TiO}_2$ and *V. faba* under saline conditions has not been thoroughly documented. Our study bridges this gap. We delved deep into the cytological changes, providing a comprehensive assessment of how cell division, chromosomal aberrations, and DNA damage respond to $n\text{TiO}_2$ treatments under salt stress. The work focuses on genes encoding antioxidant enzymes and other protection- and growth-related genes. Understanding these mechanisms provides critical insights into how $n\text{TiO}_2$ works at the genetic level to mitigate the impacts of salinity.

In connection with the above, the purpose of this work was to investigate, from the cellular to molecular levels, how $n\text{TiO}_2$ nanoparticles influence the growth of *V. faba* under salinity stress as well as to expand the understanding of the possible mechanisms involved in the adaptation of plants from the osmotic and toxic effects of salinity and the role of nanoparticles in this adaptation.

2. Materials and Methods

2.1. Experimental Conditions and Treatments

Seeds of a salinity-sensitive cultivar of *V. faba* (Sakha 101) were used in this investigation. Seeds were procured from the Agriculture Research Centre (ARC), Giza, Egypt. The seeds were surface sterilized with 2.5% NaOCl for 2 min followed by sterile distilled water three times. The seeds were dried using sterile filter paper. Sterilized seeds were soaked in wet tissue for 48 h and then planted in pots (25 cm diameter and 35 cm height) filled with betmos. Five seedlings per pot were maintained 7 days after planting. The experiment was divided into nine groups and three replicates for each group (Table S1). One was left as a negative control, where a solution of half-strength Hoagland was used for irrigation (control), while other groups were divided into two concentrations of salinity [100 mM (S1) and 200 mM (S2) of NaCl] and two concentrations of nanotitanium ($n\text{TiO}_2$) [10 ppm (T1) and 20 ppm (T2) of $n\text{TiO}_2$]. The other four groups were used for the combination of two salinity levels with two nanotitanium dioxide concentrations—S1T1, S1T2, S2T1, and S2T2. All treatments began after 10 days of planting. Half-strength Hoagland nutrient solution was used for the preparation of all treatments. Thus, salt and nanoparticles proceeded

simultaneously with irrigation every three days, starting from the tenth day of vegetation; as a result, 7 treatments were made.

Plant samples were collected 32 days after planting for fresh measurements or stored at -80°C for further determination.

2.2. Nanotitanium Dioxide ($n\text{TiO}_2$)

Commercially available nanotitanium dioxide ($n\text{TiO}_2$) sourced from Rhawn Company, China, with an average size of 5–10 nm, was used in the current study.

2.3. Growth Parameters

Changes in fresh (FW) and dry (DW) weights were used to evaluate the growth pattern of seedlings under different conditions. The fresh weight of the whole seedling was determined after carefully washing the shoots and roots of each seedling with distilled water and gently drying them with a paper towel. Dry weight was measured by reweighting the seedling after heating in a dry oven at 105°C for 3 h. The relative water content (RWC) was calculated on the basis of Fw according to the equation $\text{RWC} = [(FW - DW)/FW] \times 100$. All measurements were carried out for 5 replicates/treatments.

2.4. Determination of Membrane Stability

Membrane stability was determined by the malondialdehyde (MDA) content and the rate of electrolyte leakage. MDA represents the equated product of lipid peroxidation in the membrane. MDA content was determined as described by Zedan and Omar [22]. Half a gram of leaf tissue was homogenized in 5 mL of 5% (*w/v*) trichloroacetic acid (TCA) and centrifuged at 4000 rpm and 5°C for 10 min. The chromogen was formed by mixing 2 mL of supernatant with 3 mL of a reaction mixture containing 20% (*w/v*) TCA and 0.5% (*w/v*) 2-thiobarbituric acid (TBA). The mixture was heated at 100°C for 15 min, and the reaction was stopped by rapid cooling in an ice-water bath, followed by centrifugation at 4000 rpm and 5°C for 10 min. The amount of MDA was measured with a spectrophotometer (UV1901PC) and was calculated using the following equation:

$$\text{MDA} = [(Abs\ 532 - Abs\ 600) - 0.0571 \times (Abs\ 450 - Abs\ 600)]/0.155$$

The rate of electrolyte leakage (EL) from fresh leaf discs was determined using a conductivity meter (Adwa-AD32, Szeged-Hungary) as described by Omar et al. [31]. Ten replicates of five leaf discs (10 mm diameter) from each treatment were taken and weighed. The discs were placed in a vial containing 20 mL of distilled water and shaken, and the electrolyte conductivity of the solution was measured immediately (EL0) and after 1 h (EL1). Finally, each vial was placed in boiling water for 1 h, left to cool to room temperature, and measured again (EL2). The leakage rate of electrolytes was calculated as the percentage of the net conductivity of the solution with leaf discs immersed for 1 h, divided by the total conductivity after boiling.

2.5. Photosynthetic Pigments

Total chlorophyll and carotenoid contents were estimated by extracting 0.1 g of fresh leaf tissue with 2 mL of 80% acetone and were assessed according to Lichtenthaler et al. [32]. The pigment estimation was performed using a spectrophotometer (UV1901PC) at 645, 663, and 470 nm, according to the method of Arnon [33].

2.6. Cytological Analysis

Root tips of the *V. faba* cultivar (Sakha 101) were used to examine the cytological responses of faba bean plants to all studied experimental conditions. Seeds with root tips of 1.5–2 cm were soaked for 48 h in solutions for all experimental treatments. Root tips were fixed in Carnoy's solution for 24 h. Root tips were then kept in 70% ethyl alcohol at 4°C until their use in slide preparation. Slides were stained with Aceto-carmine

stain (2%) as described by Kihlman [34]. Prepared slides were examined, and all mitotic phases and chromosomal aberrations were counted in at least 3000 examined cells per treatment (1000 cells/replicate) using a light microscope ($40\times$) (PT/Slope, Pearl, Milton Keynes, UK). The obtained results were used to calculate the mitotic index (MI), and the percentages of cells with chromosomal abnormalities (abnormal cells, AC) were calculated using the following formulas [19]:

$$MI = (\text{Total dividing cells}/\text{Total dividing and nondividing cells}) \times 100$$

$$AC = (\text{Total abnormal cells}/\text{Total dividing cells}) \times 100$$

2.7. Total Soluble Protein

The total soluble protein (TSP) was extracted from 0.5 g of leaf tissues with liquid nitrogen. They were pulverized without thawing and were promptly resuspended 1.5 mL of extraction buffer containing 50 mM Tricine-Tris, 1 mM ethylene diamine tetraacetic acid, 1 mM dithiothreitol, 1 mM leupeptin, 1 mM pepstatin, and 1 mM phenylmethylsulfonyl fluoride (pH 7.4). Bovine serum albumin (BSA) was used in the preparation of the protein standard to determine the concentration of extracted protein [35]. SDS-polyacrylamide gel electrophoresis (SDS-PAGE) was used to detect the changes in the protein profiling pattern according to Laemmli [36]. Fifteen micrograms of protein from each sample were loaded per lane on the gel. A prestained molecular protein ladder (BLUeye-GeneDrex) was used.

2.8. Comet Assay

The comet assay was carried out as previously described in Badawy et al. [37] to determine the potential of DNA damage induced in all experimental conditions. One gram of crushed leaves of 32-day-old plants was resuspended in 1 mL of ice-cold PBS and filtered after stirring for 5 min. Low-melting agarose in PBS (0.8%) was used to prepare coated slides. Ethidium bromide (0.1 μ g/mL) was used for slide staining at 4 °C. Slide examination was conducted while it was still humid. Migration patterns of DNA fragments in 100 cells for each sample were examined using a fluorescence microscope (Confocal microscope C2, Nikon, Tokyo, Japan) at a magnification of $40\times$ and with an excitation filter of 420–490 nm. Measuring the level of DNA damage as the length of DNA migration, the percentage of migrated DNA and tail length were detected in the examined cells. These measurements were assessed using Komet 5 image analysis software developed by Kinetic Imaging, Ltd. (Liverpool, UK) linked to a CCD camera. The length of comet tails was measured from the middle of the nucleus to the end of the tail.

2.9. Gene Expression

2.9.1. RNA Extraction and cDNA Synthesis

Total RNA was extracted from previously frozen material (leaves of 32-day-old plants). An IQeasy™ plus (USA, Kirkland WA) plant extraction kit was used to extract total RNA from 0.1 g of ground tissues in liquid nitrogen according to the user manual. The appearance of two main separated bands of RNA on a 1.0% agarose gel is the main confirmation of RNA quality and integrity. A NanoDrop spectrophotometer (BioDrop µLITE. Cambridge Research Park Beach Drive, Waterbeach Cambridge, United Kingdom) was used to determine RNA concentration and purity. RNA samples with a purity ratio greater than 1.9 were considered acceptable for gene expression analysis. Single-stranded cDNAs were synthesized from 1 μ g of total RNA using oligo (dT)18 primers and the HiSenScript™ RH cDNA synthesis kit (iNtRON Biotechnology, Seoul, Republic of Korea).

2.9.2. Real-Time PCR Analysis

Changes in the transcript levels of some stress- and growth-related genes were determined using quantitative real-time PCR (qRT-PCR). SYPER Green with low ROX

(Topreal™ qPCR 2X preMix, Enzyomics, Seoul, Republic of Korea) was used for qRT-PCR in a 20 μ L reaction volume. The reactions were run on Real-Time PCR system Applied Biosystem™ Step One Plus™ (Step One Plus™, Foster City, CA 94404, USA) Real-Time PCR system. The endogenous control for all reactions was the actin gene (accession no. JX444700.1) from *V. faba*. Gene-specific primers were designed according to available data for *V. faba* from the National Center on Biotechnology Information (NCBI) using Primer 3 online software (Table 1). Relative expression (RQ) was calculated as $2^{-\Delta\Delta Ct}$ calibrated with the endogenous control and control treatment according to Livak and Schmittgen [38]. Means \pm SEs were calculated for three biological replicates for each cDNA sample.

Table 1. List of primers used in qRT-PCR analysis.

Gene	Function	Accession No.	Sequence 5'-3'
<i>GPRP</i>	Glycine-proline-rich protein	AB615379.1	GAGGAATGCTTGCTGGAGGT AGCACCACCATGACCATAGC
<i>Actin</i>	<i>Actin</i>	JX444700.1	TGGAGATGATGCACCTCGTGC CACGCTTAGACTGTGCCTCA
<i>CAT</i>	Catalase	JQ043348.1	CGATGCTTCTGTCATGCAG CAGGTGCCAAGTCGGTAT
<i>GR</i>	Glutathion reductase	EU884307.1	AGAGTTTGATAAGGGGGAGC ACAGCCCATATGCTAGGGA
<i>Fe-SOD</i>	Iron Superoxide dismutase	EU884308.1	TGAAAGAGACTTGGTTCAGTTGA GATTGCAAGCCATGCCAG
<i>Cu/Zn-SOD</i>	Cu/Zn superoxide dismutase	EU884303.1	CCGAGGATGAGACTAGACATGC CATCAGGATCGGCATGGACA
<i>HSP-17.9</i>	Heat shock protein	KC249973.2	TCGACATGCCAGGGTTGAAA CACAGCTGAAACAGCATTGG
<i>HSP-70.1</i>	Heat shock protein	EU884304	GACCACCGGTCAGAAGAAC ACCCGCATTATCCTCAGACT
<i>PSII-D1</i>	Chloroplast psbA	X17694.2	TGCTGCCCTCCAGTAGATA CAAACCGATGACCGCAGAAG

2.10. Statistics

Each plant leaf of the middle tier fixed in liquid nitrogen was treated as a biological replicate; thus, three biological replicates were performed to determine dry weight, membrane stability, photosynthetic pigment content, comet assay, gene expression, and total soluble protein (TSP) unless otherwise specified. For each of these experiments, at least three parallel independent measurements were taken. The significance of differences between groups was calculated using a one-way analysis of variance (ANOVA) followed by Duncan's method using Statistical Package for Social Sciences (SPSS) software version 20.0.1.0. Letters indicate significant differences between variants ($p < 0.05$) unless otherwise specified. Data are given as arithmetic means \pm standard errors.

3. Results

3.1. Growth Parameters

The results of the growth parameter analysis showed that both levels of salinity (S1 and S2) had a severe impact on the values of fresh and dry weights and water content (WC) (Figure 1). The values of FW, DW, and WC decreased by 14.2, 9.5, and 5.4%, respectively, under treatment with 200 mM of NaCl (S2), compared with plants under control conditions. Both concentrations of nTiO₂ (T1 and T2) induced a significant increase in Fw values in stressed and nonstressed plants (Figure 1A). The addition of nTiO₂ to stressed plants led to an increase in DW and WC values, and these increases were significant in plants treated with higher levels of salinity (S2T1 and S2T2) compared to stressed plants without nTiO₂ treatment (Figure 1B,C).

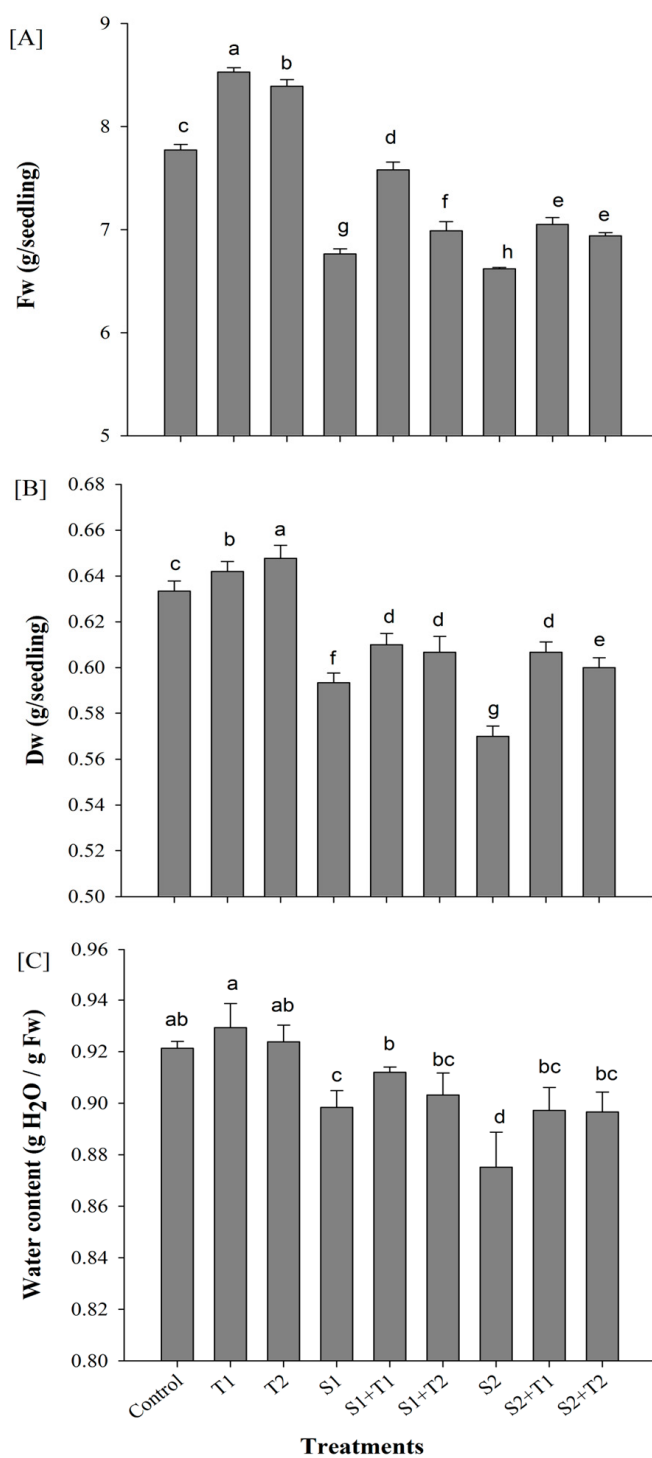


Figure 1. Changes in fresh weight (FW) (A), dry weight (DW) (B), and water content (WC) (C) in *V. faba* seedlings under all experimental conditions. Control: irrigated with half-strength Hoagland's solution, T1: 10 ppm of nTiO₂ in half-strength Hoagland's solution, T2: 20 ppm of nTiO₂ in half-strength Hoagland's solution, S1: 100 mM of NaCl in half-strength Hoagland's solution, S1T1: 100 mM of NaCl + 10 ppm of nTiO₂ in half-strength Hoagland's solution, S1T2: 100 mM of NaCl + 20 ppm of nTiO₂ in half-strength Hoagland's solution, S2: 200 mM of NaCl in half-strength Hoagland's solution; S2T1: 200 mM of NaCl + 10 ppm of nTiO₂ in half-strength Hoagland's solution, and S2T2: 200 mM of NaCl + 20 ppm of nTiO₂ in half-strength Hoagland's solution. Different letters denote statistically significant differences in mean values at $p < 0.05$ (ANOVA followed by Duncan's method) between experimental treatments.

3.2. Biochemical Determinations

3.2.1. Membrane Stability

Determination of the percentage of electron leakage (%) and the content of lipid peroxidation products (Figure 2) revealed that both levels of salinity (S1 and S2) induced significant increases in MDA content (Figure 2A) and leakage percentage (Figure 2B) when compared to those in unstressed plants. Both concentrations of nTiO₂ (T1 and T2) induced a significant reduction in the values of MDA (Figure 2A) and leakage percentage (Figure 2B) in both stressed and unstressed plants compared to untreated plants. The results indicate that treatment with 10 ppm of nTiO₂ (T1) had a better effect on alleviating oxidative stress at both levels of salinity, as shown by the values of MDA and the leakage rate.

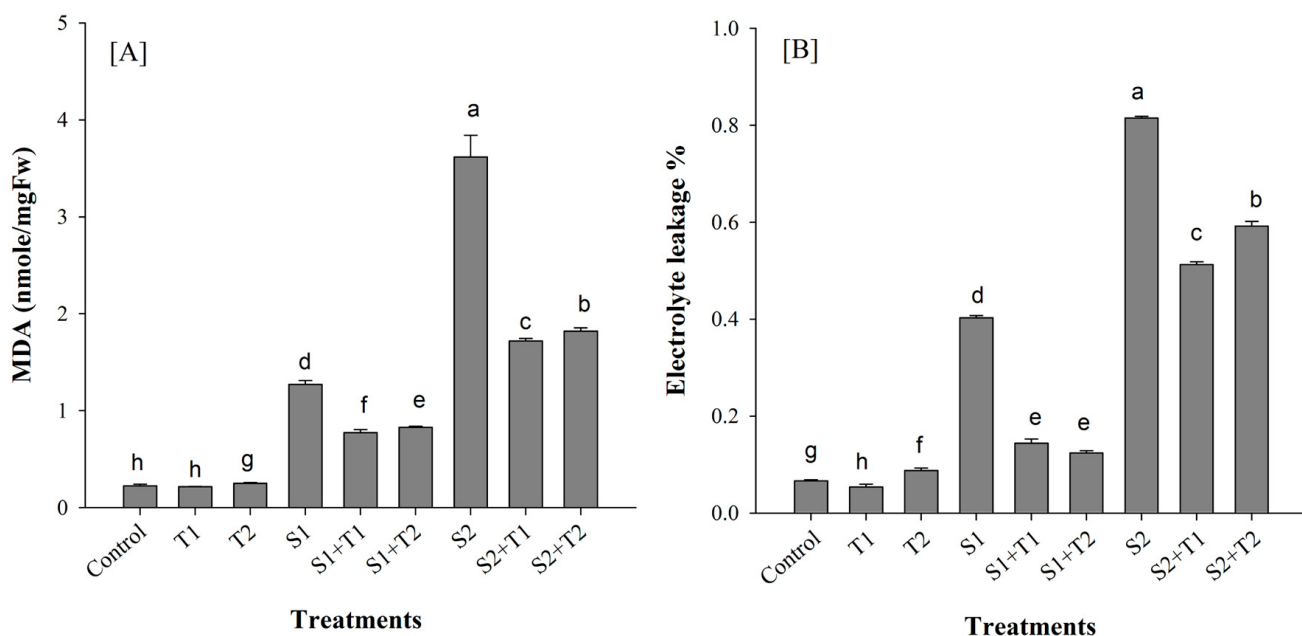


Figure 2. Changes in MDA content (A) and leakage rate of electrolyte (B) in *V. faba* seedlings under all experimental conditions. Control: irrigated with half-strength Hoagland's solution, T1: 10 ppm of nTiO₂ in half-strength Hoagland's solution, T2: 20 ppm of nTiO₂ in half-strength Hoagland's solution, S1: 100 mM of NaCl in half-strength Hoagland's solution, S1T1: 100 mM of NaCl + 10 ppm of nTiO₂ in half-strength Hoagland's solution, S1T2: 100 mM of NaCl + 20 ppm of nTiO₂ in half-strength Hoagland's solution, S2: 200 mM of NaCl in half-strength Hoagland's solution, S2T1: 200 mM of NaCl + 10 ppm of nTiO₂ in half-strength Hoagland's solution, and S2T2: 200 mM of NaCl + 20 ppm of nTiO₂ in half-strength Hoagland's solution. Different letters denote statistically significant differences in mean values at $p < 0.05$ (ANOVA followed by Duncan's method) between experimental treatments.

3.2.2. Photosynthetic Pigments

Determination of total chlorophyll and carotenoid contents as an indicator of the efficiency of the photosynthesis process revealed that plants under both salinity levels (S1 and S2) exhibited significant reductions in the values of total chlorophyll and carotenoids compared to unstressed plants (control, T1 and T2) (Figure 3). The reduction in both pigments was approximately 50% of its values in plants under control conditions. The addition of nTiO₂ induced a significant increase in total chlorophyll and carotenoid values in unstressed plants. This increase was significant for both levels of nTiO₂ treatments under both levels of salinity (S1 and S2) compared to untreated, stressed plants. The positive effects of nTiO₂ on photosynthetic pigments were significant under both levels of salinity (S1 and S2).

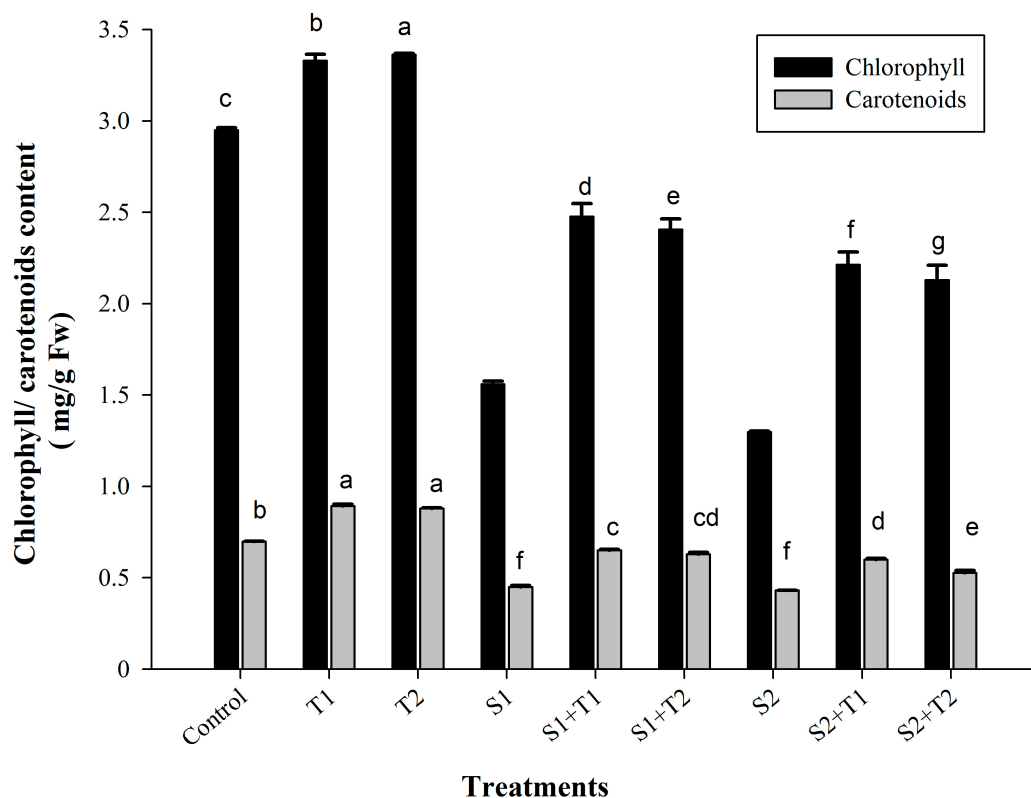


Figure 3. Changes in total chlorophyll and carotenoid contents in *V. faba* seedlings under all experimental conditions. Control: irrigated with half-strength Hoagland's solution, T1: 10 ppm of nTiO₂ in half-strength Hoagland's solution, T2: 20 ppm of nTiO₂ in half-strength Hoagland's solution, S1: 100 mM of NaCl in half-strength Hoagland's solution, S1+T1: 100 mM of NaCl + 10 ppm of nTiO₂ in half-strength Hoagland's solution, S2: 200 mM of NaCl in half-strength Hoagland's solution; S1+T2: 100 mM of NaCl + 20 ppm of nTiO₂ in half-strength Hoagland's solution, S2+T1: 200 mM of NaCl + 10 ppm nTiO₂ in half-strength Hoagland's solution, and S2+T2: 200 mM of NaCl + 20 ppm of nTiO₂ in half-strength Hoagland's solution. Different letters denote statistically significant differences in mean values at $p < 0.05$ (ANOVA followed by Duncan's method) between experimental treatments.

3.2.3. Total Soluble Proteins

The banding pattern of separated proteins on SDS-PAGE showed a series of changes in band number and density among all tested samples. Both levels of salinity caused the loss of some high- and low-molecular-weight bands (indicated with arrows) (Figure 4). Treatments with both concentrations of nTiO₂ showed a good recovery for all lost bands and induced new bands. Analysis of the banding pattern using a gel analyser program showed that the total number of separated bands was 15 bands under control conditions (Table 2). Percentages of induced and lost bands were calculated for each treatment compared with separated bands in the control treatment. Both salinity concentrations (S1 and S2) caused losses in bands. Approximately 6.67% of the total number of separated bands was lost under the lowest salt concentration (S1). The percentage of lost bands was increased to 26.67% in the S2 treatments. The number of separated bands increased by 13.33% in unstressed plants treated with both concentrations of nTiO₂. The percentage of induced bands ranged from 0 to 26.67 in stressed plants treated with both concentrations of nTiO₂ (Table 2).

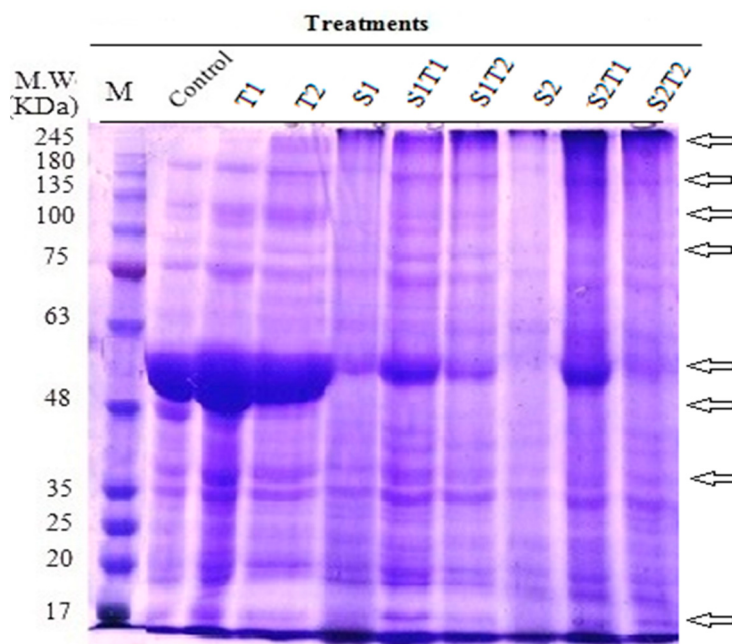


Figure 4. SDS-PAGE of separated bands of total soluble proteins extracted from *V. faba* seedlings under all experimental conditions. Arrows indicate the lost and induced bands. Control: irrigated with half-strength Hoagland's solution, T1: 10 ppm of nTiO₂ in half-strength Hoagland's solution, T2: 20 ppm of nTiO₂ in half-strength Hoagland's solution, S1: 100 mM of NaCl in half-strength Hoagland's solution, S1T1: 100 mM of NaCl + 10 ppm of nTiO₂ in half-strength Hoagland's solution, S1T2: 100 mM of NaCl + 20 ppm of nTiO₂ in half-strength Hoagland's solution, S2: 200 mM of NaCl in half-strength Hoagland's solution; S2T1: 200 mM of NaCl + 10 ppm of nTiO₂ in half-strength Hoagland's solution, and S2T2: 200 mM of NaCl + 20 ppm of nTiO₂ in half-strength Hoagland's solution.

Table 2. Changes in the number and percentage of total soluble protein separated bands on SDS-PAGE.

Treatments	Control	T1	T2	S1	S1 + T1	S1 + T2	S2	S2 + T1	S2 + T2
Total number of separated bands	15	17	17	14	19	15	11	16	18
% of changes in band no.	+ 13.33	+ 13.33	- 6.67	+ 26.67	0.00	+ 26.67	- 6.67	+ 6.67	+ 20.00

Control: irrigated with half-strength Hoagland's solution, T1: 10 ppm of nTiO₂ in half-strength Hoagland's solution, T2: 20 ppm of nTiO₂ in half-strength Hoagland's solution, S1: 100 mM of NaCl in half-strength Hoagland's solution, S1T1: 100 mM of NaCl + 10 ppm of nTiO₂ in half-strength Hoagland's solution, S1T2: 100 mM of NaCl + 20 ppm of nTiO₂ in half-strength Hoagland's solution, S2: 200 mM of NaCl in half-strength Hoagland's solution, S2T1: 200 mM of NaCl + 10 ppm of nTiO₂ in half-strength Hoagland's solution, and S2T2: 200 mM of NaCl + 20 ppm of nTiO₂ in half-strength Hoagland's solution. (-/+ indicates a loss or increase in band numbers.

3.3. Cytological Study

This study aimed to assess the possible changes in the cell division rate and chromosomal abnormalities associated with salinity conditions and to determine the potential mitigating role of nTiO₂ in the adverse effects of salinity. The data shown in Table 3 revealed that the mitotic activity of salt-stressed seedlings was significantly inhibited where salinity caused a decrease in the number of cells entering mitotic division from 119 divided cells under the control treatment to 6 and 31 under the first (S1) and second (S2) levels of salinity, respectively. The mitodepressive effect of salt interferes with the normal process of mitosis and causes a decrease in the number of dividing cells, subsequently resulting in a significant reduction in MI. The addition of nTiO₂ to salinity-treated seedlings adjusted the mitotic

inhibition of the cell cycle and reduced the number of dividing cells. In comparison to the control, the percentages of the metaphase stages increased under the first concentration of salinity. Our results showed that the S2T2 treatment showed a holistic change in the percentage of phases in comparison with the control, with a decrease in prophases and an increase in telophases (Table 3). The highest value of MI was scored at the highest level of nTiO₂ (T2), followed by S1T1, T1, and S2T2; they showed significant ($p < 0.05$) differences compared with the negative (control, T1 and T2)

Table 3. Effect of salt stress and nTiO₂ on the mitotic index (MI) and chromosomal abnormalities in *V. faba* seedlings.

Treatments	Total No. of Examined Cells	No. of Dividing Cells	No. of Abnormal Cells	Mitotic Phase (%)				Mitotic Index (%)	Abnormalities (%)
				Prophase	Metaphase	Anaphase	Telophase		
control	3367	119	0	59.66	3.36	21.85	15.12	3.56 ± 1.24 c	0.00 ± 0.00
S1	3000	6	0	0	50	16.66	33.33	0.20 ± 0.17 e	0.00 ± 0.00
S2	3169	31	0	64.52	9.68	16.67	9.68	0.95 ± 0.91 d	0.00 ± 0.00
T1	3154	226	8	56.64	4.87	11.50	26.99	7.13 ± 1.39 ab	3.25 ± 1.89
T2	3118	259	8	69.49	8.11	7.34	15.10	8.35 ± 1.08 a	2.92 ± 2.53
S1T1	3152	215	1	57.21	6.05	11.16	25.58	7.17 ± 0.85 ab	0.44 ± 0.76
S2T1	3125	118	11	63.02	14.41	11.02	13.56	3.78 ± 0.38 c	0.00 ± 0.00
S1T2	2913	79	1	45.57	1.27	45.57	7.59	2.71 ± 0.95 cd	1.33 ± 2.30
S2T2	3075	183	5	33.88	12.57	6.01	47.54	6.07 ± 1.73 b	2.56 ± 4.43
Sig.								0.00	0.24

Control: irrigated with half-strength Hoagland's solution, T1: 10 ppm of nTiO₂ in half-strength Hoagland's solution, T2: 20 ppm of nTiO₂ in half-strength Hoagland's solution, S1: 100 mM of NaCl in half-strength Hoagland's solution, S1T1: 100 mM of NaCl + 10 ppm of nTiO₂ in half-strength Hoagland's solution, S1T2: 100 mM of NaCl + 20 ppm of nTiO₂ in half-strength Hoagland's solution, S2: 200 mM of NaCl in half-strength Hoagland's solution; S2T1: 200 mM of NaCl + 10 ppm of nTiO₂ in half-strength Hoagland's solution, and S2T2: 200 mM of NaCl + 20 ppm of nTiO₂ in half-strength Hoagland's solution. Different letters denote statistically significant differences in mean values at $p < 0.05$.

Salt treatments showed the lowest value in MI, whereas S2T1 and S1T2 did not differ from the control treatment. Regarding chromosomal aberrations, several types of chromosomal abnormalities were recorded in all studied treatments (Figure 5). There were no significant differences between treatments. The highest ratio was recorded in T1, followed by T2. Therefore, nTiO₂ recorded a high ratio of aberrations, but this ratio was not significant.

3.4. Comet Assay

A comet assay was carried out to assess DNA breaking in stressed and unstressed seedlings of *V. faba* with and without nTiO₂ treatments. Induced DNA damage appears as breaks and increased fragmentation (Figure 6A). The analysis of the comet assay results (Figure 6) showed that both levels of salinity (S1 and S2) prompted a significant increase in DNA damage ($p < 0.05$), as evidenced by a rise in the tailed nuclei percentage (Figure 6B) and an increase in tail length (μm) (Figure 6C) compared to the three control groups (control, T1 and T2). The elevation in DNA damage in stressed plants was recovered after treatment with nTiO₂. Significant reductions in the % of tailed nuclei and tail length were recorded in stressed plants treated with both levels of nTiO₂ compared to untreated stressed plants. The best recovery was observed with the second concentration of nTiO₂ with the first level of salinity (S1T2). The reduction effect of nTiO₂ on DNA breaks remained significantly higher than that in the control groups. No significant difference was noticed between the negative control and the two nTiO₂ concentration treatments. In our results, the salt induced damage

to the DNA of *V. faba* seedlings; this damage was reduced following treatment with both concentrations of nTiO₂. Treatment with 20 ppm of nTiO₂ (T2) was the best in inducing the recovery of salinity effects.

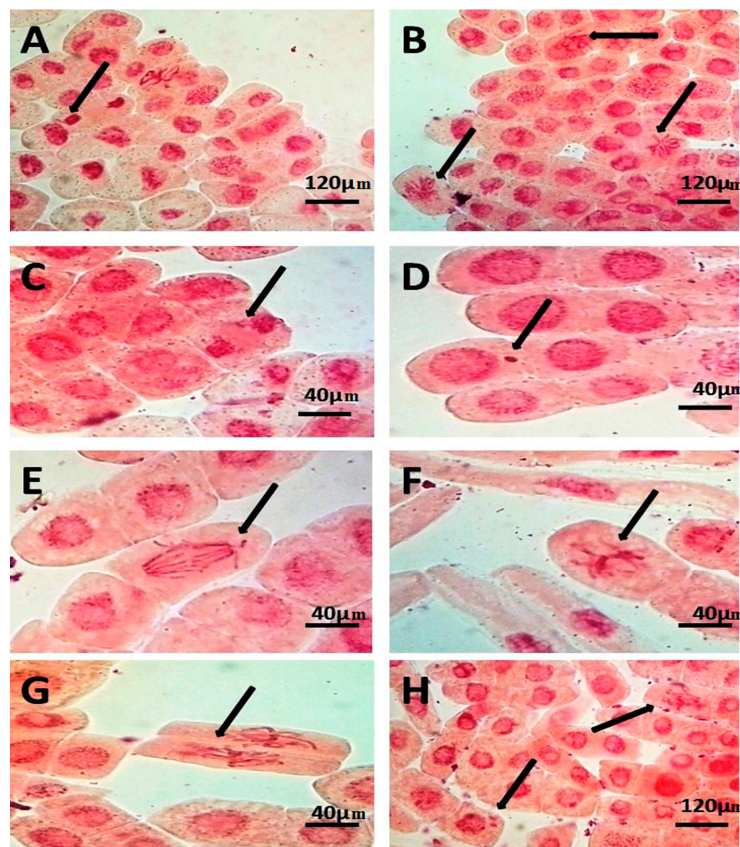


Figure 5. All types of chromosomal abnormalities were scored during cytological examination of root tips from *V. faba* seedlings under all experimental conditions. Scored abnormalities included (A): sticky telophase, (B): condensed and sticky chromosome and unoriented chromosome, (C): lagging chromosome, (D): micronuclei, and (E): anaphase with forward lagging chromosome. (F): Sticky metaphase with disturbed chromosome. (G): Disturbed metaphase. (H): Sticky and unoriented chromosome and double micronuclei. Arrows pointed to cells with recorded abnormalities.

3.5. Gene Expression Analysis

Transcript expressions for some stress- and growth-related genes were studied using a qRT-PCR analysis. Our experiment included the determination of the expression of some antioxidant enzymes encoding genes, such as superoxide dismutase (Fe-SOD or Cu/Zn-SOD); glutathione reductase (GR) and catalase (CAT); some protection protein genes, such as heat shock proteins (HSP17.9 and HSP70), and growth-related genes, such as photosystem II-D protein (PSII-D1; and glycine- and proline-rich protein-encoding genes (GPRP). Our results (Figure 7) showed that both levels of salinity (S1 and S2) induced a significant reduction in the transcript expression of all studied genes (Figure 7), except for Fe-SOD and Cu/Zn-SOD (Figure 7A,B) when compared to control seedlings. In contrast, the relative expression of Fe-SOD and Cu/Zn-SOD (Figure 7A,B) showed a significant increase under the first level of salinity (S1), while it dropped significantly in plants with the second level of salinity (S2). The application of both concentrations of nTiO₂ (T1 and T2) elicited marked increments in the studied gene expressions, whether in stressed or unstressed plants. Given that HSP17.9 and HSP70 function as molecular chaperones pivotal for cellular component protection, they were incorporated in this evaluation. In our study, the two nTiO₂ levels (T1 and T2) triggered a significant upsurge in HSP17.9 and HSP70 in unstressed plants (Figure 7E,F). Despite both salinity levels inducing a notable reduction in

these genes, nTiO₂ treatment led to a significant boost in their transcript counts, doubling in treated stressed plants compared to those untreated with nTiO₂ (Figure 7E,F). The PSII-D1-encoding gene, a core subunit of photosystem II (PSII) and particularly susceptible to salinity stress in our study, witnessed significant downregulation under both salinity levels (S1 and S2). In contrast, its expression was enhanced notably by 1.2- and 1.54-fold under the two nTiO₂ levels (T1 and T2). We also evaluated the glycine- and proline-rich protein (GPRP)-encoding gene (*GPRP*), postulated to play crucial roles in plant growth and development. Our data (Figure 7H) showed a marked reduction in *GPRP* transcripts under both salinity levels (S1 and S2). Conversely, both nTiO₂ concentrations significantly augmented the *GPRP*-encoding gene expression, up to 4.38- and 3.909-fold, respectively. In salinity-stressed plants, nTiO₂ treatment substantially amplified *GPRP* transcription, reaching nearly threefold under the second nTiO₂ level (T2), compared to its untreated counterpart. Collectively, our findings stress the pivotal role of nTiO₂ in mediating both stress and growth responses in *V. faba* under varying salinity conditions. Treatment of stressed plants with nTiO₂ significantly stimulated the transcription of *GPRP* to almost twofold under the first level of salinity (S1) and approximately twofold under the second level of salinity (S2) (Figure 7H).

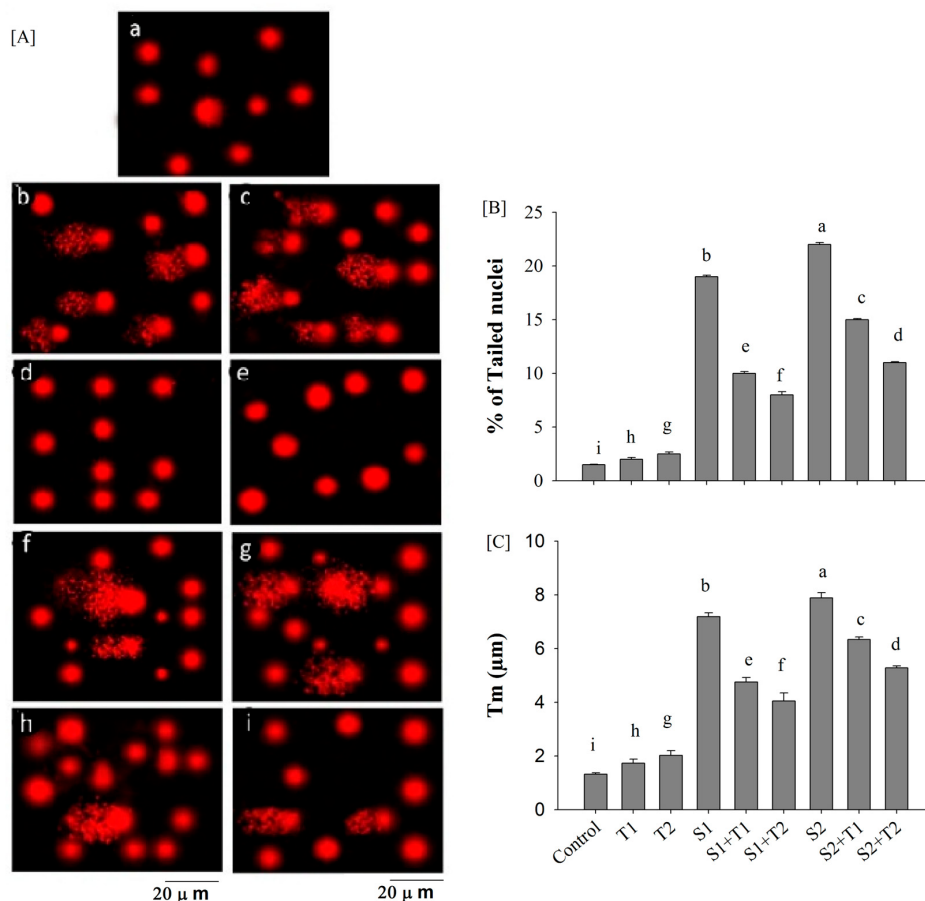


Figure 6. DNA genotoxicity of leaf nuclei from *V. faba* under different experimental treatments. **(A)**: Representative images of the plant cells assayed via the comet assay where (a): control; (b): salinity of 100 mM (S1); (c): salinity of 200 mM (S2); (d): nTiO₂ of 10 ppm (T1); (e): nTiO₂ of 20 ppm (T2); (f): salinity of 100 mM + nTiO₂ of 10 ppm (S1T1); (g): salinity of 200 S2; (h): salinity of 200 mM + nTiO₂ of 10 ppm (S2T1); and (i): salinity of 200 + nTiO₂ of 20 ppm (S2T2). **(B)** Percentage of tailed nuclei of examined seedlings under all experimental conditions. **(C)** Mean tail length (μm). Slides were examined with a magnification of 40× and with an excitation filter of 420–490 nm. Different letters denote statistically significant differences in mean values at $p < 0.05$ (ANOVA followed by Duncan's method) between experimental treatments.

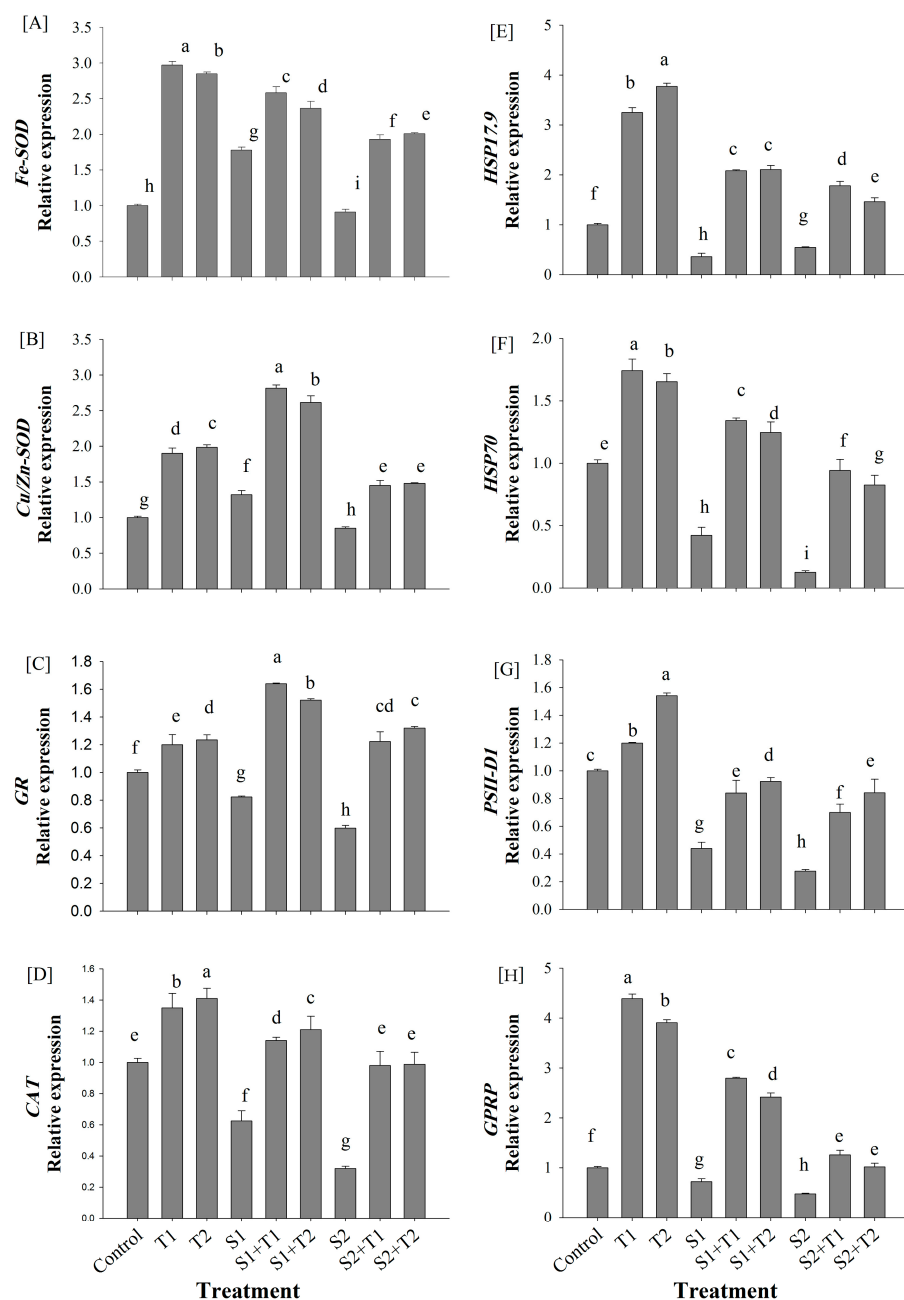


Figure 7. Changes in the expression level of some stress and growth responsive genes *Fe-SOD* (A), *Cu/Zn-SOD* (B), *GR* (C), *CAT* (D), *HSP 17.9* (E), *HSP 70* (F), *PSII-D1* (G) and *GPRP* (H) in *V. faba* seedlings under all experimental conditions. The expression was determined as changes in the transcript amount using qRT-PCR. Relative expression (RQ) was calculated as $2^{-\Delta\Delta Ct}$ calibrated with the endogenous gene (accession no. JX444700.1) and control treatment as endogenous control. Data are given as the means \pm SEs of relative expression for three biological replicates for each cDNA sample. Control: irrigated with half-strength Hoagland's solution, T1: 10 ppm of nTiO₂ in half-strength Hoagland's solution, T2: 20 ppm of nTiO₂ in half-strength Hoagland's solution, S1: 100 mM of NaCl in half-strength Hoagland's solution, S1+T1: 100 mM of NaCl + 10 ppm of nTiO₂ in half-strength Hoagland's solution, S1+T2: 100 mM of NaCl + 20 ppm of nTiO₂ in half-strength Hoagland's solution, S2: 200 mM of NaCl in half-strength Hoagland's solution; S2+T1: 200 mM of NaCl + 10 ppm of nTiO₂ in half-strength Hoagland's solution, and S2+T2: 200 mM of NaCl + 20 ppm of nTiO₂ in half-strength Hoagland's solution. Different letters denote statistically significant differences in mean values at $p < 0.05$ (ANOVA followed by Duncan's method) between experimental treatments.

4. Discussion

Applications of NPs are considered a promising strategy to overcome the difficulties of plant growth and production under oxidative stress. Assessment of their impacts on plants and investigation of the associated changes in treated plants are needed. In this study, the most prominent changes associated with salinity stress were the significant reduction in growth parameters of *V. faba* plants. The reduction in FW, DW, WC, and photosynthesis pigments was observed under both studied levels of salinity (Figures 1 and 3). The association of growth reduction with salinity conditions is known in many plant species [39,40]. The mitotic index is a valid metric for determining cellular division frequency and assessing cytotoxicity [41]. In our studies, the use of nanoparticles significantly restored the mitotic indices that had been reduced due to salt stress (Table 3). These results explain the delay in growth parameters under salinity conditions as a result of cell division inhibition and the reduction in prophase indices [42].

The inhibition of some physiological and biochemical processes due to decreasing metabolic activity and the massive production of reactive oxygen species (ROS) cause a growth reduction under salinity conditions [29,43]. Oxidative stress generated by salt stress causes peroxidation of membrane lipids (Figure 2A), subsequently damaging the membrane features. Loss of membrane permeability increases the leakage rate of electrolytes [29,44]. A reduction in photosynthetic activity under salinity stress has been recorded in many plant species [45,46]. This was also confirmed by our experiments (Figure 2B). Salinity stress causes a large decrease in stomatal conductance, which leads to a reduction in CO₂ concentration and a reduction in the net photosynthetic rate [47,48]. Treated unstressed and stressed plants with both concentrations of nTiO₂ induced a significant improvement in growth and biochemical parameters compared with untreated plants (Figures 1 and 3). The stimulatory effects of nTiO₂ on root and shoot growth by enhancing plant metabolism and cell division were reported [43]. Recovery effects of nTiO₂ on stressed plants were recorded in tobacco [29]. These effects highlighted the physiological role of nTiO₂ in increasing light harvesting, activation of photosynthesis, and stimulation of protein and pigment content [49]. Considering our results and other documented results, the application of nTiO₂ at different concentrations increased total biomass, photosynthetic pigments, plant growth, and plant performance under stress compared to untreated plants [29,43,49,50] (Figures 1–3).

Regarding previous studies and recent results, the recovery effects of nTiO₂ could be explained. It was stated that the foliar application of nTiO₂ protects the chloroplast from ageing and prolongs its photosynthesis time [51]. The stability of chlorophyll and carotenoid content was recorded in plants under cold stress as a result of nTiO₂ treatment [52]. Stimulation of Rubisco carboxylase activity enhances chlorophyll content and raises the photosynthetic rate in the presence of nTiO₂ [53,54]. nTiO₂ treatments control the activities of enzymes involved in nitrogen metabolism and enhance the conversion process of inorganic nitrogen to organic nitrogen and the synthesis of proteins and chlorophyll [14,51]. nTiO₂ improves the synthesis of NO, which has previously been reported to enhance carbonic anhydrase (CA) enzyme activity [5]. The enhanced activity of CA maintained constant CO₂ access to the Rubisco enzyme, thus leading to an improvement in the rate of carbon assimilation and an improved photosynthesis process and, consequently, growth rate.

High production of reactive oxygen species (ROS) under stress conditions causes degradation and irreversible damage to protein structures and loss of their functions [29,55]. The role of nTiO₂ in the stimulation of nitrogen metabolism by increasing the absorption of nitrate and accelerating the conversion rate of the inorganic form of nitrogen helps in protein conservation and induction [6], which may explain its recovery effects on the band pattern of TSP separated on SDS-PAGE (Figure 4; Table 2). A protein with a size of approximately 55 kDa was specifically enriched in the control; T1, T2, S1T1, and S2T1 samples (Figure 4). We hypothesize that at higher NaCl concentrations (200 mM), it might induce a stronger stress response compared to the control or nTiO₂ concentrations. Moreover, it cannot be

ruled out that the nanoparticles themselves may also influence the accumulation of this protein, which is quite intriguing. This stress can lead to changes in protein synthesis and degradation, resulting in altered levels of specific proteins.

It is possible that at certain concentrations, nTiO₂ might help plants cope with salt stress through various mechanisms, such as enhancing antioxidant activity or improving nutrient uptake [30]. NPs are involved in the upregulation of antioxidant enzyme activities such as superoxide dismutase (Fe-SOD and Cu/Zn-SOD), catalase (CAT), and peroxidases (POD) [43]. It was recorded that nTiO₂ induces alterations in plant redox status in some plant species [56,57]; these alterations were not identical and depended on the plant species and the exposure conditions [57,58]. The stimulatory effect of nTiO₂ on antioxidant enzyme activities (POX, Cu/Zn-SOD, CAT, APX, and GR) was reported in faba beans under water deficit stress compared with untreated stressed plants [59]. Although the effect of nTiO₂ on enzyme activity was reported in different species, our results are one of the rare studies that confirm these responses at the transcript level of antioxidant-encoding genes. The upregulation of antioxidant enzyme-encoding genes by nTiO₂ (Figure 7) could explain the reduction in the oxidative load of ROS in stressed plants [55]. This supports the recovery role of nTiO₂ either on membrane properties or for damaged DNA. Damaged DNA assessed using a comet assay indicated a significant reduction in tailed nuclei and tail length in stressed plants treated with nTiO₂ (Figure 6B,C). To the best of our knowledge, our result is the first record of the use of the comet assay technique to assess the recovery effects of nanomaterial application on salinity stress. Both concentrations of nTiO₂ induced recovery of damaged DNA under both levels of salinity. Ruffini Castiglione [60] indicated that increased doses of TiO₂ cause an increase in DNA fragmentation.

The up-regulation role of nTiO₂ for some stress- and growth-related genes was confirmed using a qRT-PCR analysis. The up-regulation of HSPs (HSP17.9 and HSP70) supports the recovery role of nTiO₂ in stressed plants (Figure 7E,F). These proteins (HSP17.9 and HSP70) play important roles in the protection of cell components and support the correct folding of newly synthesized proteins, as they work as molecular chaperones and prevent the aggregation of misfolded proteins [61,62]. One of the other genes upregulated by nTiO₂ treatment is the PSII-D1-protein-encoding gene. It is a key subunit of photosystem II (PSII) and collaborates with the D2 protein to bind all the redox-active cofactors required in the process of energy conversion and is considered the main target of light-induced photo-oxidation [63]. Previous studies reported the influence of abiotic stress on PSII extrinsic proteins and damage to the D1 protein [64]. From our results, we infer that photosynthesis recovery induced by nTiO₂ treatments could occur as a result of induced activation of antioxidant enzymes (Figure 7A–D), which play a significant role in the reduction of photo-oxidative stress in addition to the stimulatory role of nTiO₂ on the transcript amount of the PSII-D1-encoding gene (Figure 7F) [65].

Our investigation also considered the changes in the transcript amount of the glycine- and proline-rich protein (GPRP)-encoding gene (GPRP). It has been proposed to play essential roles in the growth and development of plants, in addition to playing a role in environmental adaptation [65,66]. It was reported that GPRPs interact with catalases and regulate their activity in response to both biotic and abiotic stresses [67,68]. Catalase activity could efficiently remove excessive H₂O₂ released under stress conditions. Therefore, the up-regulation of GPRPs in stressed plants treated with nTiO₂ is associated with the recovery of plant performance under oxidative stress. To the best of our knowledge, this is the first record of the role of NPs in stimulating the expression of GPRPs, which could help in understanding the mechanisms of the positive effects of nTiO₂ on plant growth under abiotic stress conditions (Figure 7H).

The stimulatory effect of nTiO₂ on the defence system and its role in the upregulation of gene expression could be proposed as a result of its role in nitric oxide (NO) generation. NO acts as a second messenger in signalling transfer and induces responses in plants subjected to biotic and abiotic stresses [23,69,70]. Moreover, nTiO₂ significantly influenced the expression pattern of microRNAs (miRNAs), which are considered important gene

regulators and play a significant role in plant tolerance to abiotic stresses [43]. Considering that timely stimulation of defence systems prior to the onset of damage is critical for plant survival under oxidative stress conditions as shown in our obtained results, it is highly recommended to apply nTiO₂ as a strategy for improving the plant growth of stressed and unstressed plants.

Finally, we can assume that nTiO₂ is able to bind with some toxic ions, mitigating or exacerbating their effects. It would be reasonable to study whether nTiO₂ plays any role in the dynamics of sodium or chloride ions in a plant under salt stress.

It is also conceivable that the combined effects of salt stress and nTiO₂ might be antagonistic. These antagonistic effects could be influenced by both the concentration and size of the nanoparticles. While nanoparticles may offer promise in shielding plants from the osmotic and toxic effects of salinity, their potential is not boundless. Beyond a certain threshold, the nanoparticles could become toxic themselves.

5. Conclusions

This study underscores the potential of nTiO₂ to enhance plant performance under saline conditions. Cytological and comet assay analyses confirmed mitigation in the adverse effects of salinity on chromosome abnormalities and DNA damage when cotreated with nTiO₂. The nanoparticles' influence was reflected in a decline in MDA content and in the dampening of the effects of salinity. This attenuation was evident in the efflux of electrolytes, shifts in the concentration of photosynthetic pigments, alterations in the ratios of water-to-dry matter, and the clear differentiation of bands for total soluble proteins. Moreover, nTiO₂ markedly modulated the expression of antioxidant enzyme-encoding genes (Fe-SOD, Cu/Zn-SOD, GR, and CAT), chaperone heat shock protein genes (HSP17.9 and HSP70), and the PSII-D-protein-encoding gene. This modulation is instrumental in bolstering plant resistance to the toxic and osmotic stresses induced by salinity.

The innovation of this research stems from its comprehensive methodology, offering a thorough investigation into the protective effects of titanium oxide nanoparticles on *V. faba* plants. These findings lay the foundation for an enriched understanding of nanoparticle effects, pivotal for elucidating the underlying mechanisms of nanoparticle interactions in future studies.

In the broader context, the economic viability of employing NPs must be addressed; while the initial costs may be higher, the long-term benefits to plant health and yield could justify the investment, particularly in regions where salinity is a persistent challenge.

Supplementary Materials: The following supporting information can be downloaded at <https://www.mdpi.com/article/10.3390/horticulturae9091030/s1>, Table S1: description of experimental treatments.

Author Contributions: Conceptualization, S.A.O., N.I.E. and A.M.Z.; methodology, S.A.O. and A.M.Z.; software, S.A.O. and P.P.; validation, S.A.O., V.K. and P.P.; formal analysis, S.A.O., P.P., S.I.A. and A.M.Z.; investigation, S.A.O., P.P., S.I.A. and A.M.Z.; resources, S.A.O., P.P., S.I.A. and A.M.Z.; writing—original draft preparation, S.A.O., P.P., S.I.A. and A.M.Z.; writing—review and editing, S.A.O., P.P., V.K., S.I.A. and A.M.Z.; visualization, S.A.O.; project administration, S.A.O., N.I.E. and S.I.A. All authors have read and agreed to the published version of the manuscript.

Funding: This study is supported by the Tanta University Competitive Project Unit (TU-03-13-06) granted to Nabil Elsheery. The results (Tables 2 and 3) were obtained within the state assignment of the Ministry of Science and Higher Education of the Russian Federation (projects no.: 122042700044-6 and 122050400128-1, respectively).

Data Availability Statement: The datasets generated during and/or analysed during the current study are available from the corresponding author upon reasonable request.

Conflicts of Interest: The authors declare no conflict of interest.

References

1. Silva, S.; Oliveira, H.; Silva, A.; Santos, C. The cytotoxic targets of anatase or rutile+ anatase nanoparticles depend on the plant species. *Biol. Plant.* **2017**, *61*, 717–725. [[CrossRef](#)]
2. Tang, X.; Mu, X.; Shao, H.; Wang, H.; Brestic, M. Global plant-responding mechanisms to salt stress: Physiological and molecular levels and implications in biotechnology. *Crit. Rev. Biotechnol.* **2015**, *35*, 425–437. [[CrossRef](#)] [[PubMed](#)]
3. Petretto, G.L.; Urgeghe, P.P.; Massa, D.; Melito, S. Effect of salinity (NaCl) on plant growth, nutrient content, and glucosinolate hydrolysis products trends in rocket genotypes. *Plant Physiol. Biochem.* **2019**, *141*, 30–39. [[CrossRef](#)]
4. Abdelaal, S.M.; Moussa, K.F.; Ibrahim, A.H.; Mohamed, E.S.; Kucher, D.E.; Savin, I.; Abdel-Fattah, M.K. Mapping Spatial Management Zones of Salt-Affected Soils in Arid Region: A Case Study in the East of the Nile Delta, Egypt. *Agronomy* **2021**, *11*, 2510. [[CrossRef](#)]
5. Kim, Y.H.; Khan, A.L.; Waqas, M.; Shim, J.K.; Kim, D.H.; Lee, K.Y.; Lee, I.J. Silicon application to rice root zone influenced the phytohormonal and antioxidant responses under salinity stress. *J. Plant Growth Regul.* **2014**, *33*, 137–149. [[CrossRef](#)]
6. Murillo-Amador, B.; Yamada, S.; Yamaguchi, T.; Rueda-Puente, E.; Ávila-Serrano, N.; García-Hernández, J.; López-Aguilar, R.; Troyo-Díéguez, E.; Nieto-Garibay, A. Influence of calcium silicate on growth, physiological parameters and mineral nutrition in two legume species under salt stress. *J. Agron. Crop Sci.* **2007**, *193*, 413–421. [[CrossRef](#)]
7. Wang, M.; Wang, Y.; Zhang, Y.; Li, C.; Gong, S.; Yan, S.; Li, G.; Hu, G.; Ren, H.; Yang, J. Comparative transcriptome analysis of salt-sensitive and salt-tolerant maize reveals potential mechanisms to enhance salt resistance. *Genes Genom.* **2019**, *41*, 781–801. [[CrossRef](#)]
8. Zhang, X.; Liu, P.; Qing, C.; Yang, C.; Shen, Y.; Ma, L. Comparative transcriptome analyses of maize seedling root responses to salt stress. *PeerJ* **2021**, *9*, e10765. [[CrossRef](#)]
9. Rahate, K.A.; Madhumita, M.; Prabhakar, P.K. Nutritional composition, anti-nutritional factors, pretreatments-cum-processing impact and food formulation potential of faba bean (*Vicia faba* L.): A comprehensive review. *LWT* **2021**, *138*, 110796. [[CrossRef](#)]
10. Bachmann, M.; Kuhnitzsch, C.; Martens, S.D.; Steinhöfel, O.; Zeyner, A. Control of bean seed beetle reproduction through cultivar selection and harvesting time. *Agric. Ecosyst. Environ.* **2020**, *300*, 107005. [[CrossRef](#)]
11. Segers, A.; Dumoulin, L.; Megido, R.C.; Jacquet, N.; Cartrysse, C.; Kamba, P.M.; Pierreux, J.; Richel, A.; Blecker, C.; Francis, F. Varietal and environmental effects on the production of faba bean (*Vicia faba* L.) seeds for the food industry by confrontation of agricultural and nutritional traits with resistance against *Bruchus* spp. (Coleoptera: Chrysomelidae, Bruchinae). *Agric. Ecosyst. Environ.* **2022**, *327*, 107831. [[CrossRef](#)]
12. Farooq, M.; Gogoi, N.; Hussain, M.; Barthakur, S.; Paul, S.; Bharadwaj, N.; Migdadi, H.M.; Alghamdi, S.S.; Siddique, K.H. Effects, tolerance mechanisms and management of salt stress in grain legumes. *Plant Physiol. Biochem.* **2017**, *118*, 199–217. [[CrossRef](#)]
13. Flexas, J.; Bota, J.; Loreto, F.; Cornic, G.; Sharkey, T. Diffusive and metabolic limitations to photosynthesis under drought and salinity in C3 plants. *Plant Biol.* **2004**, *6*, 269–279. [[CrossRef](#)] [[PubMed](#)]
14. Mishra, V.; Mishra, R.K.; Dikshit, A.; Pandey, A.C. Interactions of nanoparticles with plants: An emerging prospective in the agriculture industry. In *Emerging Technologies and Management of Crop Stress Tolerance*; Elsevier: Amsterdam, The Netherlands, 2014; pp. 159–180. [[CrossRef](#)]
15. Filippou, P.; Bouchagier, P.; Skotti, E.; Fotopoulos, V. Proline and reactive oxygen/nitrogen species metabolism is involved in the tolerant response of the invasive plant species *Ailanthus altissima* to drought and salinity. *Environ. Exp. Bot.* **2014**, *97*, 1–10. [[CrossRef](#)]
16. Gohari, G.; Mohammadi, A.; Akbari, A.; Panahirad, S.; Dadpour, M.R.; Fotopoulos, V.; Kimura, S. Titanium dioxide nanoparticles (TiO₂ NPs) promote growth and ameliorate salinity stress effects on essential oil profile and biochemical attributes of *Dracocephalum moldavica*. *Sci. Rep.* **2020**, *10*, 912. [[CrossRef](#)] [[PubMed](#)]
17. Duhan, J.S.; Kumar, R.; Kumar, N.; Kaur, P.; Nehra, K.; Duhan, S. Nanotechnology: The new perspective in precision agriculture. *Biotechnol. Rep.* **2017**, *15*, 11–23. [[CrossRef](#)] [[PubMed](#)]
18. Mekuye, B.; Abera, B. Nanomaterials: An overview of synthesis, classification, characterization, and applications. *Nano Select.* **2023**, *4*, 463–524. [[CrossRef](#)]
19. Das, A.; Das, B. Nanotechnology a potential tool to mitigate abiotic stress in crop plants. *Abiotic Biot. Stress Plants* **2019**. [[CrossRef](#)]
20. Abdel Latef, A.A.H.; Abu Alhmad, M.F.; Abdelfattah, K.E. The possible roles of priming with ZnO nanoparticles in mitigation of salinity stress in lupine (*Lupinus termis*) plants. *J. Plant Growth Regul.* **2017**, *36*, 60–70. [[CrossRef](#)]
21. Marchiol, L.; Mattiello, A.; Pošćić, F.; Fellet, G.; Zavalloni, C.; Carlino, E.; Musetti, R. Changes in physiological and agronomical parameters of barley (*Hordeum vulgare*) exposed to cerium and titanium dioxide nanoparticles. *Int. J. Environ. Res. Public Health* **2016**, *13*, 332. [[CrossRef](#)]
22. Zedan, A.; Omar, S. Nano Selenium: Reduction of severe hazards of Atrazine and promotion of changes in growth and gene expression patterns on *Vicia faba* seedlings. *Afr. J. Biotechnol.* **2019**, *18*, 502–510. [[CrossRef](#)]
23. Khan, M.N.; Mobin, M.; Abbas, Z.K.; AlMutairi, K.A.; Siddiqui, Z.H. Role of nanomaterials in plants under challenging environments. *Plant Physiol. Biochem.* **2017**, *110*, 194–209. [[CrossRef](#)] [[PubMed](#)]
24. Sharma, S.; Singh, V.K.; Kumar, A.; Mallubhotla, S. Effect of Nanoparticles on Oxidative Damage and Antioxidant Defense System in Plants. In *Molecular Plant Abiotic Stress: Biology and Biotechnology*; Wiley: Hoboken, NJ, USA, 2019; pp. 315–333. [[CrossRef](#)]
25. Ye, Y.; Medina-Velo, I.A.; Cota-Ruiz, K.; Moreno-Olivas, F.; Gardea-Torresdey, J.L. Can abiotic stresses in plants be alleviated by manganese nanoparticles or compounds? *Ecotoxicol. Environ. Saf.* **2019**, *184*, 109671. [[CrossRef](#)] [[PubMed](#)]

26. Zhu, Y.-X.; Gong, H.-J.; Yin, J.-L. Role of silicon in mediating salt tolerance in plants: A review. *Plants* **2019**, *8*, 147. [CrossRef]
27. Liu, K.; Cao, M.; Fujishima, A.; Jiang, L. Bioinspired titanium dioxide materials with special wettability and their applications. *Chem. Rev.* **2014**, *114*, 10044–10094. [CrossRef] [PubMed]
28. Chutipajit, S.; Sutjaritvorakul, T. Application of activated charcoal and nanocarbon to callus induction and plant regeneration in aromatic rice (*Oryza sativa* L.). *Chem. Speciat. Bioavailab.* **2018**, *30*, 1–8. [CrossRef]
29. Khan, M.N. Nanotitanium dioxide (nano-TiO₂) mitigates NaCl stress by enhancing antioxidative enzymes and accumulation of compatible solutes in tomato (*Lycopersicon esculentum* Mill.). *J. Plant Sci.* **2016**, *11*, 1–11. [CrossRef]
30. Van Aken, B. Gene expression changes in plants and microorganisms exposed to nanomaterials. *Curr. Opin. Biotechnol.* **2015**, *33*, 206–219. [CrossRef]
31. Omar, S.A.; Elsheery, N.I.; Kalaji, H.M.; Xu, Z.-F.; Song-Quan, S.; Carpentier, R.; Lee, C.-H.; Allakhverdiev, S.I. Dehydroascorbate reductase and glutathione reductase play an important role in scavenging hydrogen peroxide during natural and artificial dehydration of *Jatropha curcas* seeds. *J. Plant Biol.* **2012**, *55*, 469–480. [CrossRef]
32. Lichtenthaler, H.K.; Wellburn, A.R. Determinations of total carotenoids and chlorophylls a and b of leaf extracts in different solvents. *Biochem. Soc. Trans.* **1983**, *11*, 591–592. [CrossRef]
33. Arnon, D.I. Copper enzymes in isolated chloroplasts. Polyphenoloxidase in Beta vulgaris. *Plant Physiol.* **1949**, *24*, 1. [CrossRef] [PubMed]
34. Kihlman, B. Root tips of Vicia faba for the study of the induction of chromosomal aberrations. *Mutat. Res. Environ. Mutagen. Relat. Subj.* **1975**, *31*, 401–412. [CrossRef]
35. Bradford, M.M. A rapid and sensitive method for the quantitation of microgram quantities of protein utilizing the principle of protein-dye binding. *Anal. Biochem.* **1976**, *72*, 248–254. [CrossRef] [PubMed]
36. Laemmli, U.K. Cleavage of structural proteins during the assembly of the head of bacteriophage T4. *Nature* **1970**, *227*, 680–685. [CrossRef]
37. Badawy, A.A.; El-Magd, M.A.; AlSadrah, S.A. Therapeutic effect of camel milk and its exosomes on MCF7 cells in vitro and in vivo. *Integr. Cancer Ther.* **2018**, *17*, 1235–1246. [CrossRef]
38. Livak, K.J.; Schmittgen, T.D. Analysis of relative gene expression data using real-time quantitative PCR and the $2^{-\Delta\Delta CT}$ method. *Methods* **2001**, *25*, 402–408. [CrossRef]
39. Negrão, S.; Schmöckel, S.; Tester, M. Evaluating physiological responses of plants to salinity stress. *Ann. Bot.* **2017**, *119*, 1–11. [CrossRef]
40. Rahneshan, Z.; Nasibi, F.; Moghadam, A.A. Effects of salinity stress on some growth, physiological, biochemical parameters and nutrients in two pistachio (*Pistacia vera* L.) rootstocks. *J. Plant Interact.* **2018**, *13*, 73–82. [CrossRef]
41. Fernandes, T.C.; Mazzeo, D.E.C.; Marin-Morales, M.A. Mechanism of micronuclei formation in polyploidized cells of Allium cepa exposed to trifluralin herbicide. *Pestic. Biochem. Physiol.* **2007**, *88*, 252–259. [CrossRef]
42. Singh, D.; Roy, B.K. Salt stress affects mitotic activity and modulates antioxidant systems in onion roots. *Braz. J. Bot.* **2016**, *39*, 67–76. [CrossRef]
43. Frazier, T.P.; Burkewell, C.E.; Zhang, B. Titanium dioxide nanoparticles affect the growth and microRNA expression of tobacco (*Nicotiana tabacum*). *Funct. Integr. Genom.* **2014**, *14*, 75–83. [CrossRef] [PubMed]
44. Qados, A.M.A. Effect of salt stress on plant growth and metabolism of bean plant *Vicia faba* (L.). *J. Saudi Soc. Agric. Sci.* **2011**, *10*, 7–15. [CrossRef]
45. Redondo-Gómez, S.; Mateos-Naranjo, E.; Davy, A.J.; Fernández-Muñoz, F.; Castellanos, E.M.; Luque, T.; Figueroa, M.E. Growth and photosynthetic responses to salinity of the salt-marsh shrub *Atriplex portulacoides*. *Ann. Bot.* **2007**, *100*, 555–563. [CrossRef]
46. Stepien, P.; Johnson, G.N. Contrasting responses of photosynthesis to salt stress in the glycophyte *Arabidopsis* and the halophyte *Thellungiella*: Role of the plastid terminal oxidase as an alternative electron sink. *Plant Physiol.* **2009**, *149*, 1154–1165. [CrossRef] [PubMed]
47. Chaves, M.; Flexas, J.; Pinheiro, C. Photosynthesis under drought and salt stress: Regulatory mechanisms from whole plant to cell. *Ann. Bot.* **2009**, *103*, 551–560. [CrossRef]
48. James, R.A.; Rivelli, A.R.; Munns, R.; von Caemmerer, S. Factors affecting CO₂ assimilation, leaf injury and growth in salt-stressed durum wheat. *Funct. Plant Biol.* **2002**, *29*, 1393–1403. [CrossRef]
49. Phothi, R.; Theerakarunwong, C.D. Enhancement of rice (*Oryza sativa* L.) physiological and yield by application of nano-titanium dioxide. *Aust. J. Crop Sci.* **2020**, *14*, 1157–1161. [CrossRef]
50. Zhou, Y.; Zhang, L.; Liu, Y.; She, J. Effects of Liquid Phase Nano Titanium Dioxide (TiO₂) on Seed Germination and Seedling Growth of Camphor Tree. *Nanomaterials* **2022**, *12*, 1047. [CrossRef]
51. Yang, F.; Hong, F.; You, W.; Liu, C.; Gao, F.; Wu, C.; Yang, P. Influence of nanoanatase TiO₂ on the nitrogen metabolism of growing spinach. *Biol. Trace Elem. Res.* **2006**, *110*, 179–190. [CrossRef]
52. Mohammadi, R.; Maali-Amiri, R.; Mantri, N. Effect of TiO₂ nanoparticles on oxidative damage and antioxidant defense systems in chickpea seedlings during cold stress. *Russ. J. Plant Physiol.* **2014**, *61*, 768–775. [CrossRef]
53. Akbari, G.-A.; Morteza, E.; Moaveni, P.; Alahdadi, I.; Bihamta, M.-R.; Hasanloo, T. Pigments apparatus and anthocyanins reactions of borage to irrigation, methylalchol and titanium dioxide. *Int. J. Biosci.* **2014**, *4*, 192–208. [CrossRef]
54. Yamori, W.; Masumoto, C.; Fukayama, H.; Makino, A. Rubisco activase is a key regulator of non-steady-state photosynthesis at any leaf temperature and, to a lesser extent, of steady-state photosynthesis at high temperature. *Plant J.* **2012**, *71*, 871–880. [CrossRef] [PubMed]

55. Jaleel, C.A.; Gopi, R.; Kishorekumar, A.; Manivannan, P.; Sankar, B.; Panneerselvam, R. Interactive effects of triadimefon and salt stress on antioxidative status and ajmalicine accumulation in *Catharanthus roseus*. *Acta Physiol. Plant.* **2008**, *30*, 287–292. [[CrossRef](#)]
56. Jahan, S.; Alias, Y.B.; Bakar, A.F.B.A.; Yusoff, I.B. Toxicity evaluation of ZnO and TiO₂ nanomaterials in hydroponic red bean (*Vigna angularis*) plant: Physiology, biochemistry and kinetic transport. *J. Environ. Sci.* **2018**, *72*, 140–152. [[CrossRef](#)]
57. Tiwari, M.; Sharma, N.C.; Fleischmann, P.; Burbage, J.; Venkatachalam, P.; Sahi, S.V. Nanotitania exposure causes alterations in physiological, nutritional and stress responses in tomato (*Solanum lycopersicum*). *Front. Plant Sci.* **2017**, *8*, 633. [[CrossRef](#)]
58. Hurum, D.C.; Agrios, A.G.; Gray, K.A.; Rajh, T.; Thurnauer, M.C. Explaining the enhanced photocatalytic activity of Degussa P25 mixed-phase TiO₂ using EPR. *J. Phys. Chem. B* **2003**, *107*, 4545–4549. [[CrossRef](#)]
59. Khan, M.N.; AlSolami, M.A.; Basahi, R.A.; Siddiqui, M.H.; Al-Huqail, A.A.; Abbas, Z.K.; Siddiqui, Z.H.; Ali, H.M.; Khan, F. Nitric oxide is involved in nanotitanium dioxide-induced activation of antioxidant defense system and accumulation of osmolytes under water-deficit stress in *Vicia faba* L. *Ecotoxicol. Environ. Saf.* **2020**, *190*, 110152. [[CrossRef](#)]
60. Ruffini Castiglione, M.; Giorgetti, L.; Geri, C.; Cremonini, R. The effects of nano-TiO₂ on seed germination, development and mitosis of root tip cells of *Vicia narbonensis* L. and *Zea mays* L. *J. Nanoparticle Res.* **2011**, *13*, 2443–2449. [[CrossRef](#)]
61. Timperio, A.M.; Egidi, M.G.; Zolla, L. Proteomics applied on plant abiotic stresses: Role of heat shock proteins (HSP). *J. Proteom.* **2008**, *71*, 391–411. [[CrossRef](#)]
62. Tichá, T.; Samakovli, D.; Kuchařová, A.; Vavrdová, T.; Šamaj, J. Multifaceted roles of HEAT SHOCK PROTEIN 90 molecular chaperones in plant development. *J. Exp. Bot.* **2020**, *71*, 3966–3985. [[CrossRef](#)]
63. Komenda, J. Role of two forms of the D1 protein in the recovery from photoinhibition of photosystem II in the cyanobacterium *Synechococcus* PCC 7942. *Biochim. Biophys. Acta (BBA)-Bioenerg.* **2000**, *1457*, 243–252. [[CrossRef](#)]
64. Nath, K.; Jajoo, A.; Poudyal, R.S.; Timilsina, R.; Park, Y.S.; Aro, E.-M.; Nam, H.G.; Lee, C.-H. Towards a critical understanding of the photosystem II repair mechanism and its regulation during stress conditions. *FEBS Lett.* **2013**, *587*, 3372–3381. [[CrossRef](#)] [[PubMed](#)]
65. Li, Y.; Chen, L.; Mu, J.; Zuo, J. LESION SIMULATING DISEASE1 interacts with catalases to regulate hypersensitive cell death in *Arabidopsis*. *Plant Physiol.* **2013**, *163*, 1059–1070. [[CrossRef](#)]
66. Li, J.; Liu, J.; Wang, G.; Cha, J.-Y.; Li, G.; Chen, S.; Li, Z.; Guo, J.; Zhang, C.; Yang, Y. A chaperone function of NO CATALASE ACTIVITY1 is required to maintain catalase activity and for multiple stress responses in *Arabidopsis*. *Plant Cell* **2015**, *27*, 908–925. [[CrossRef](#)] [[PubMed](#)]
67. Halder, T.; Upadhyaya, G.; Roy, S.; Biswas, R.; Das, A.; Bagchi, A.; Agarwal, T.; Ray, S. Glycine rich proline rich protein from Sorghum bicolor serves as an antimicrobial protein implicated in plant defense response. *Plant Mol. Biol.* **2019**, *101*, 95–112. [[CrossRef](#)] [[PubMed](#)]
68. Liu, X.; Wang, X.; Yan, X.; Li, S.; Peng, H. The Glycine-and Proline-Rich Protein AtGPRP3 Negatively Regulates Plant Growth in *Arabidopsis*. *Int. J. Mol. Sci.* **2020**, *21*, 6168. [[CrossRef](#)] [[PubMed](#)]
69. Cao, X.; Zhu, C.; Zhong, C.; Zhang, J.; Wu, L.; Jin, Q.; Ma, Q. Nitric oxide synthase-mediated early nitric oxide burst alleviates water stress-induced oxidative damage in ammonium-supplied rice roots. *BMC Plant Biol.* **2019**, *19*, 108. [[CrossRef](#)]
70. Huang, M.; Ai, H.; Xu, X.; Chen, K.; Niu, H.; Zhu, H.; Sun, J.; Du, D.; Chen, L. Nitric oxide alleviates toxicity of hexavalent chromium on tall fescue and improves performance of photosystem II. *Ecotoxicol. Environ. Saf.* **2018**, *164*, 32–40. [[CrossRef](#)]

Disclaimer/Publisher's Note: The statements, opinions and data contained in all publications are solely those of the individual author(s) and contributor(s) and not of MDPI and/or the editor(s). MDPI and/or the editor(s) disclaim responsibility for any injury to people or property resulting from any ideas, methods, instructions or products referred to in the content.